Journal of Applied Polymer Science

Aliphatic Polycarbonate-Based Polyurethane Elastomers and Nanocomposites. II. Mechanical, Thermal, and Gas Transport Properties

Rafał Poręba,[1] Milena Špírková,[1] Libuše Brožová,[2] Nada Lazić,[3] Jelena Pavličević,[1,*] Adam Strachota[1]

[1]Nanostructured Polymers and Composites Department, Institute of Macromolecular Chemistry AS CR v.v.i, (IMC), Heyrovsky Sq. 2, Prague 162 06, Czech Republic

[2]Polymer Membrane Department, IMC, Prague 162 06, Czech Republic

[3]Institute of General and Physical Chemistry, Belgrade 11000, Serbia

*Present address: Faculty of Technology, Department of Materials Engineering, University of Novi Sad, Bul. Cara Lazara 1, 21000 Novi Sad, Serbia

Correspondence to: M. Špírková (E-mail: spirkova@imc.cas.cz)

ABSTRACT: Thermal, thermomechanical, tensile and gas transport properties of aliphatic polycarbonate-based polyurethanes (PC-PUs) and their nanocomposites with bentonite for organic systems were studied. Hard segments are formed from hexamethylene diisocyanate and butane-1,4-diol. All PC-PUs and their nanocomposites feature high degree of the phase separation. Three phase transitions were detected by temperature-modulated differential scanning calorimetry (TMDSC) and dynamic mechanical thermal analysis. TMDSC revealed the filler affinity both to soft and hard segments, even though the affinity to hard segments is much stronger. Elongation-at-break at ambient temperatures is mostly over 700%, which leads together with high tensile strength (in some cases) to very high toughness values (over 200 mJ/mm^3). The addition of 1 wt % of bentonite does not practically affect mechanical properties implying its very good incorporation into the PU matrix. Permeabilities and other gas transport properties depend on regularity of PC-diol and on hard segment content, but the variations are insignificant. © 2012 Wiley Periodicals, Inc. J. Appl. Polym. Sci. 000: 000–000, 2012

KEYWORDS: polyurethane elastomer; nanocomposite; polycarbonate diol; bentonite; hydrogen bonds

Received 28 December 2011; accepted 14 April 2012; published online
DOI: 10.1002/app.37895

INTRODUCTION

The polyurethane (PU) elastomers are multiple block copolymers composed of hard (glassy) and soft (rubbery) segments. They form segregated two-phase structures of the nanometer size at room temperatures as a result of the incompatibility of different segments. For hard segment contents (HSC) lower than 50%, the hydrogen-bond-containing hard segment domains (HSD) act as physical crosslinks dispersed in the soft-segment matrices.[1,2] While the soft segments (SS) secure sufficient flexibility, the hard domains (formed by the reaction of the diisocyanate and the chain extender) provide high cohesive strength of PU materials due to strong intermolecular interaction (hydrogen bonding) inside hard segments (HS) of urethane linkages. If additional hydrogen bonds between soft and hard phases are formed (which depends mainly on the chemical structure of HS and SS), a fairly high degree of phase mixing can be expected. However, the mixing and the overall microstructure of the PUs depend also on other factors such as the block length, macrodiol molecular weight, the HS/SS ratio, the crystallinity of domains, their incompatibility, and thermal history.

Thermal analysis (e.g., DSC) has been often used to yield information on structural transitions in polymer systems, such as glass transitions, melting, and crystallization processes, to understand their mechanical properties in a wide temperature range.[3–11] Three phase transitions in the temperature range from –70 to 200°C are typical for PU elastomers containing less than 50% of HS: The transition at the lowest temperature (mostly between –70 and –20°C) corresponds to the glass/rubber transition of the soft segments. The other transitions are located between 50 to 80°C and 120 to 200°C (denoted as endotherm I and II). Their full and unambiguous interpretation has not yet been finished, though both endothermic processes

have been intensively studied for several decades and several hypotheses have been proposed: Endotherm I (region 50–80°C) have been ascribed, e.g., to the disruption of short-range HS ordering,[3,4] melting of HS domains,[5] breaking up of the less ordered noncrystalline hard-segment-domains,[6] short-range ordering of hard segment domains as a result of the annealing and quenching,[7] hard-segment disordering in the boundary region between soft and hard phases,[8] the relaxation of chain segments in the diffused interface between soft and hard segment domains[9,10] or to transitions in domains of soft segments especially if contents of soft segment is high.[6] Endotherm II (120–200°C) has been assigned e.g., to the disruption (break-up) of long-range hard segment ordering,[2,3,6] the disruption of various degree of short-range HS ordering,[11] melting of microcrystalline HSD[6] or order-disorder transition of hard segment microdomains.[9]

The conventional DSC does not often yield sufficient information, especially if several processes overlap in a narrow temperature range. The disadvantage of conventional DSC has been recently overcome with the temperature-modulated differential scanning calorimetry (TMDSC), which employs small sinusoidal heating, and cooling waves superimposed on the linear heating or cooling ramp.[12] In comparison to DSC, the TMDSC technique enables a decomposition of the total heat flow in a reversible (thermal) and nonreversible (kinetic) component.[13] TMDSC was recently used for successful thermal analysis of PUs and PU nanocomposites[9,10,14–16] and it is also used in this article.

Besides calorimetry, the mechanical thermal analysis (both static and dynamic) is other frequently used method for the characterization of PC-PU elastomers and nanocomposites.[5,6,10,16–21] It not only yields important pieces of information that can be directly compared with results of calorimetry studies, but it provides also information of mechanical properties of prepared materials. As one of principal goals of this study was the preparation of materials with suitable application properties, we have been using this technique as a principal tool of investigation.

So far, the aromatic diisocyanates have been mostly used in the PU formulations[5,17–20] but some PC-PUs based on aliphatic isocyanates, mainly HDI[6,10,16,21] have been applied as well. The aim of this article is a detailed thermo-mechanical study of end-use properties of a series of samples that we prepared recently (and characterized from the molecular up to micrometer level by a combination of spectroscopy (NMR, IR), scattering (SAXS, WAXD) and microscopy techniques).[22] Gas transport properties of prepared PC-PUs are compared with that of commercial available PC-PUs. The influence of the type of the isocyanate (aliphatic/aromatic) and the length of the polycarbonate diol chain (M_w 1000 and 2000) on thermal and mechanical properties is discussed as well.

EXPERIMENTAL

Materials and Preparation Procedure

All-aliphatic polycarbonate macrodiols with molecular weight ca. 2000 (PCDL T5652, PCDL T4672 and PCDL T4692; marked as 5652, 4672, and 4692), were kindly provided by Asahi Kasei Chemical Corporation, Tokyo, Japan. The characteristics of macrodiols (MD) were given by the supplier: 5652 OH value: 57.0 mg KOH/g, water content: 0.0043 wt %, viscosity at 50°C: 9970 mPa s; 4672 OH value: 54.2 mg KOH/g, water content 0.0077 wt %, viscosity at 50°C: 18300 mPa s; 4692 OH value: 55.8 mg KOH/g, water content 0.0185 wt %, viscosity at 70°C: 6410 mPa s. Hexamethylene diisocyanate (HDI, purum, $\geq$ 98%), butane-1,4-diol (BD; purum, $\geq$ 98 chain extender) and the catalyst, dibutyltin dilaurate (DBTDL; all Fluka, Buchs, Schweiz) were used as received. The catalyst solution was prepared in oil Marcol (20%). The modified bentonite (bentonite for organic systems, BO, Fluka) was used as filler.

All PU samples were prepared by one step technique. The isocyanate index, $r = [NCO]/[OH]$ was kept constant 1.05 in all cases. The ratio $R = [OH]_{MD}/[OH]_{BD}$ varied from 0.3 to ∞. $R = \infty$ means PU samples prepared without any chain extender (BD). Catalyst concentration, c_{DBTDL}, was kept at 0.005 wt %. The mixture containing macrodiol, chain extender and catalyst was degassed. Then diisocyanate was added in the reaction mixture, mixed, again degassed, and poured into Teflon molds. The samples containing the filler (PU-clay nanocomposites) were prepared by the same procedure, when a full dispersion of nanofiller (bentonite, BO) was achieved by 1 day swelling in macrodiol and butanediol mixture, and by subsequent brief stirring for 10 min of the mixture, before addition of isocyanate. Samples were kept in nitrogen atmosphere at 90°C for 24 h. For all PC-PU samples prepared, uniform codes were used: macrodiol type / R / wt % of BO / wt % of hard segments. Sample composition and codes are summarized in Table I.

Temperature-Modulated Differential Scanning Calorimetry (TMDSC)

The investigation of PC-PUs phase transition behavior was carried out by means of the temperature-modulated differential scanning calorimetry (MTDSC, Q1000 TA Instruments). The samples (masses of about 5 mg) were placed in sealed aluminum pans and heated from −80 to 200°C at the heating rate of 3°C/min. Dry nitrogen with a flow rate of 50 mL/min was used as a purge gas. Temperature scale and the heat flow were calibrated using an indium standard. During the experiments, a small-amplitude sinusoidal wave pattern is over-imposed on the linear heating ramp[23] and the temperature profile can be expressed as follows: $T(t) = T_0 + qt + A\sin(wt - \theta)$, where T_0 is the starting temperature, A is the amplitude of temperature oscillation, w is the modulation frequency, θ is the phase shift with respect to the reference, and q is the heating rate. The modulation temperature amplitude and oscillation period were set at ± 0.5°C and 40 s (frequency of 25 mHz), respectively. The freshly prepared samples were firstly cooled to approximately −90°C at a cooling rate of 3°C/min, and then the measurements were started. The computer software (TA Universal Analysis) was used to analyze thermal curves obtained from the first scan. The T_g values were determined from the intersect of the tangent to the low-temperature thermal expansion side with the tangent to the thermal-expansion side of the curve beyond the transition.

Dynamic Mechanical Thermal Analysis (DMTA)

Dynamic mechanical thermal analysis was carried out on ARES-LS2, Rheometrics Scientific (now TA instruments) using oscillation frequency of 1 Hz, deformation ranging from 0.01% (glassy

Table I. Codes and Composition of PC-PUs and Their Nanocomposites

Sample no.	Code	PC diol	R^a	BO (wt %)	HSC (wt %)
1	5652/0.3/0/35	5652	0.3	0	35.4
2	5652/0.4/0/30	5652	0.4	0	29.9
3	5652/0.5/0/27	5652	0.5	0	26.9
3B	5652/0.5/1/27	5652	0.5	1	26.8
4	5652/1/0/19	5652	1	0	18.7
4B	5652/1/1/19	5652	1	1	18.6
4BB	5652/1/2/19	5652	1	2	18.5
5	5652/2/0/14	5652	2	0	13.9
6	5652/10/0/9	5652	10	0	9.2
6B	5652/10/1/9	5652	10	1	9.0
7	5652/∞/0/8	5652	∞[b]	0	8.4
8	4672/0.3/0/34	4672	0.3	0	34.2
9	4672/0.5/0/26	4672	0.5	0	25.9
9B	4672/0.5/1/26	4672	0.5	1	26.0
10	4672/1/0/18	4672	1	0	17.8
10B	4672/1/1/18	4672	1	1	17.7
11	4672/2/0/13	4672	2	0	13.1
12	4672/10/0/9	4672	10	0	8.9
12B	4672/10/1/9	4672	10	1	8.9
13	4672/∞/0/8	4672	∞[b]	0	8.0
14	4692/1/0/18	4692	1	0	18.2

[a] $R = [OH]_{MD}/[OH]_{BD}$, [b] Prepared without any BD.
HSC = $(m_{HDI} + m_{BD})/(m_{HDI} + m_{BD} + m_{MD})$, where m is mass of the relevant component; expressed in wt %.

state) to 3.5% (maximum deformation allowed), over a temperature range of –100 to 180°C, at a heating rate of 3°C/min. Dynamic torsion measurements were performed using rectangular samples, to which a constant tension force of 5 g was applied. The standard specimens dimensions were 25 mm × 3 mm × 2 mm. Storage modulus (G'), loss modulus (G'') and loss factor (tan δ, tan $\delta = G''/G'$) were measured. In this work, the glass transition temperature was defined as temperature of maximum value of tan(δ).

Tensile Characterization

Static mechanical properties were measured on an Instron model 5800, Instron Limited, UK. Specimens with gauge length 25 mm were tested at 23°C at a test speed of 0.17 mm s^{-1}. The reported values are averages obtained from at least five specimens.

Gas Transport Property Measurement

Gas transport properties of samples prepared in the form of free-standing films were determined using a laboratory high-vacuum apparatus with a static permeation cell.[24] After a high vacuum was reached in the apparatus, the studied gas under constant pressure p_i higher than atmospheric was brought into the feed part of the apparatus. Permeability was determined from the increase in pressure Δp_p per the time interval Δt in a calibrated volume V_p using the formula, $P = \frac{\Delta p_p}{\Delta t} \cdot \frac{V_p l}{s p_i} \cdot \frac{1}{RT}$, where l is membrane thickness, s its area, T is temperature and R is the gas constant. The solubility coefficient was calculated as a ratio of the permeability P to the diffusion coefficient, D, i.e., $S = P/D$. The diffusion coefficient was calculated from time lag (Θ) and the membrane thickness (l) according to the equation, $D = \frac{l^2}{6\Theta}$.

Gas transport properties of oxygen, nitrogen, carbon dioxide, methane and hydrogen were studied for all PU samples. The purity of gases was higher than 99.95%. All measurements were carried out at 30°C.

RESULTS AND DISCUSSION

All studied PC-PUs are formed from bifunctional compounds (macrodiol, short diol and diisocyanate). The polyaddition reactions between isocyanate and hydroxyl groups (belonging either to macrodiol or BD) result in formation of linear polyurethane chains containing soft segments with low T_g and hard segments with high T_g. Because their miscibility is limited, a substantial phase separation occurs and segregated hard segment (HDI/BD) and soft segment (macrodiol) domains are formed.

No chemical (covalent) crosslinking takes place during the preparation used and the network joint points are of pure physical character, i.e., H-bonds between —NH— (in urethane, $NH_{urethane}$), and —C=O (in urethane, $CO_{urethane}$).* In case of

*Small amount of urea groups (reaction product of isocyanate with traces of water omnipresent in hydroxyl-containing compounds) can also be formed. As they were not detected by IR,[22] their content is omitted.

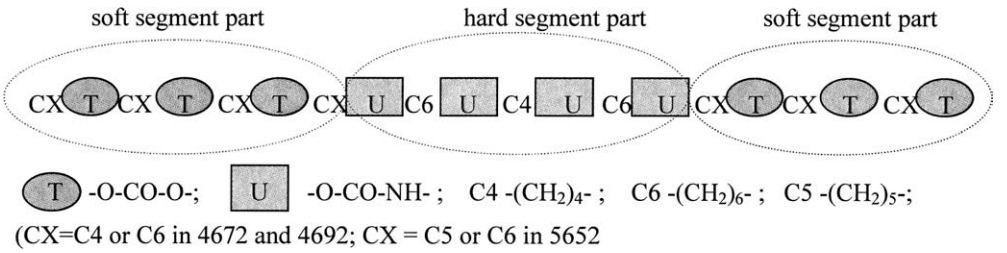

Scheme 1. The part of PC-PU chain.

polycarbonate diol used, further appreciable physical bonding in PC-PUs occurs: H-bonds between —NH— of urethane and —C=O of carbonate, $NH_{urethane} \cdots CO_{carbonate}$ form and also inter- or intramolecular dipole–dipole interactions in macrodiol chain(s) play important role.† Unlike in "common" PU elastomers, where physical crosslinking ($NH_{urethane} \cdots CO_{urethane}$) is significant only inside hard segment domains (or on the hard-soft segment domain interphase), a substantial physical bonding between hard and soft segments (interactions $NH_{urethane} \cdots CO_{carbonate}$) and inside soft segments (interactions $CO_{carbonate} \cdots CO_{carbonate}$)† exist in PC-PUs. From the experimental point of view, it is difficult to discern, separate and quantify different types of secondary bonds, i.e., to estimate their contents and strength, but they all influence macroscopic end-use properties detectable by appropriate analytical methods such as DMTA, TMDSC, tensile testing. Even though the preparation technique is a simple (one shot procedure; 24 h at 90°C) and PU chains are created from only a few sequences distributed within the PU chain: CX (X= 4 to 6), —O—CO—O— (T) and —NH—CO—O— (U) in (Scheme 1), due to the formation of different secondary bonds differing in the strength and range, the prepared PU samples exhibit complex thermo-mechanical behavior which allows for tailoring the end-use properties. A small part of PC-PU chain is depicted in Scheme 1. For further discussion, it is worth-mentioning that PC-PUs prepared from macrodiol 4672 or 4692 contain only even C4 and C6 sequences, while 5652-based PUs have even C4 and C6, and odd C5 units in their polymer chains. The 4672 and 5652 macrodiols were chosen for the detailed study because: (i) they have similar MW and hence OH contents and (ii) they contain identical number of carbonate groups in the macrodiol chain (16 on average; due to C4/C6 or C5/C6 ratio). Macrodiol 4692, containing average 18 carbonate groups in the chain, was used just for testing the effect of macrodiol C4/C6 ratio on end-use properties, and only at $R = 1$.

Prepared polyurethane products (14 PC-PUs and 7 PC-PU nanocomposites) allowed for studying of (i) the influence of the ratio R for series 4672 (samples Nos. 1 to 7 in Table I) and for series 5652 (Nos. 8–13); (ii) the influence of the macrodiol type at $R = 1$ (Nos. 4, 10, and 14); (iiia) the comparison of PU elastomer and related nanocomposite; 1 wt % (Nos. 3 vs. 3B, 4 vs. 4B, 6 vs. 6B, 9 vs. 9B, 10 vs. 10B, and 12 vs. 12B) and (iiib) the influence of bentonite concentration (0, 1, and 2 wt %—Nos.4, 4B, and 4BB in Table I) on thermal, thermomechanical, tensile and gas transport properties. All the phenomena and dependences are discussed in the following paragraphs.

Temperature-Modulated Differential Scanning Calorimetry (TMDSC)

In our recent TMDSC studies of polyurethanes made from PC diol M_W 1000, $(PC\text{-}PUs)_{1000}$, we detected three types of transitions: the glass transition of soft segments at −34 to −40°C; endothermic event located at 40–60°C, and multiple endotherms connected to the melting of hard segments at > 100°C.[10,16] The purpose of present TMDCS study is to investigate the structure of segmented PC-PU elastomers based on macrodiols with M_w ca. 2000 at the molecular and supermolecular level, and to relate the mechanical properties with phase transitions. The effect of polycarbonate diol constitution and nanoclay addition on the end-use properties and the relationship between the nanostructure (segregation) and thermo-mechanical properties are also studied and compared with previous results.[10,16]

The glass transition temperatures of PC diols were determined as the peak maxima from the derivative of the reversing heat capacity versus temperature (Figure 1). The glass transition temperatures $(T_g)_{PCD}$ were detected: −44°C (4692), −46°C (4672), and −49°C (5652) and they are in accordance with the literature DSC data.[5] PC diols 4692 and 4672 are formed purely

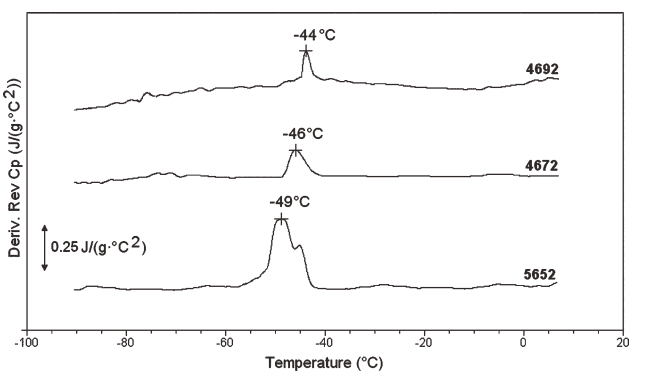

Figure 1. Temperature dependences of the differential of reversing heat capacity for PC diols 5652, 4672, and 4692.

†Polycarbonate diol contains carbonate groups regularly distributed inside the macrodiol chain. Each carbonate bonding –O–CO–O– has three oxygens with lone-pear electrons leading to the magnetic force and resulting in the packing of the carbonate bonding structure either inside one macrodiol chain (intramolecular dipole–dipole interactions) or between two macrodiol chains (intermolecular dipole–dipole interactions). This phenomenon occurs both in macrodiol and in soft-segment domains of PC-PU.

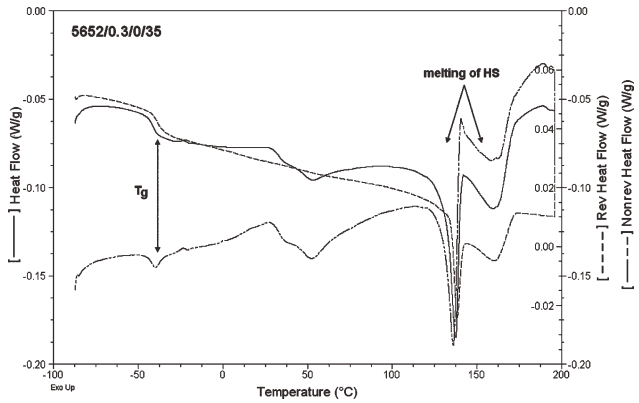

Figure 2. TMDSC curves for sample 5652/0.3/0/35.

from odd C4 and C6 units which results in almost linear configuration. Their glass transition is marked by one narrow peak only (especially sharp for the most regular PC diol 4692). Macrodiol 5652, which consists of even (C6) and odd (C5) building units, shows two peaks (second as a shoulder), i.e., its glass transition covers a certain region due to its less regular structure. Macrodiol 5652 is also more flexible than 4672 and especially 4692 and exhibits a broader glass transition region (see Figure 1.) Different macrodiol chain stiffness in individual samples was also confirmed by solid-state NMR spectroscopy;[22] TMDSC and NMR results are in a good agreement.

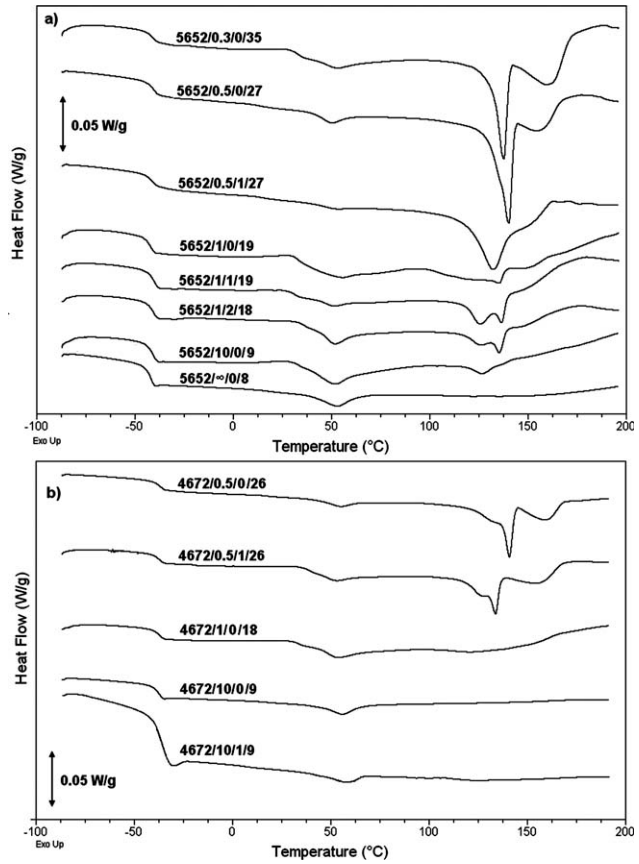

Figure 3. Total specific heat flow versus temperature dependences for polyurethanes and their nanocomposites based on (a) 5652 and (b) 4672 macrodiol. (For sample code description, see Table I.)

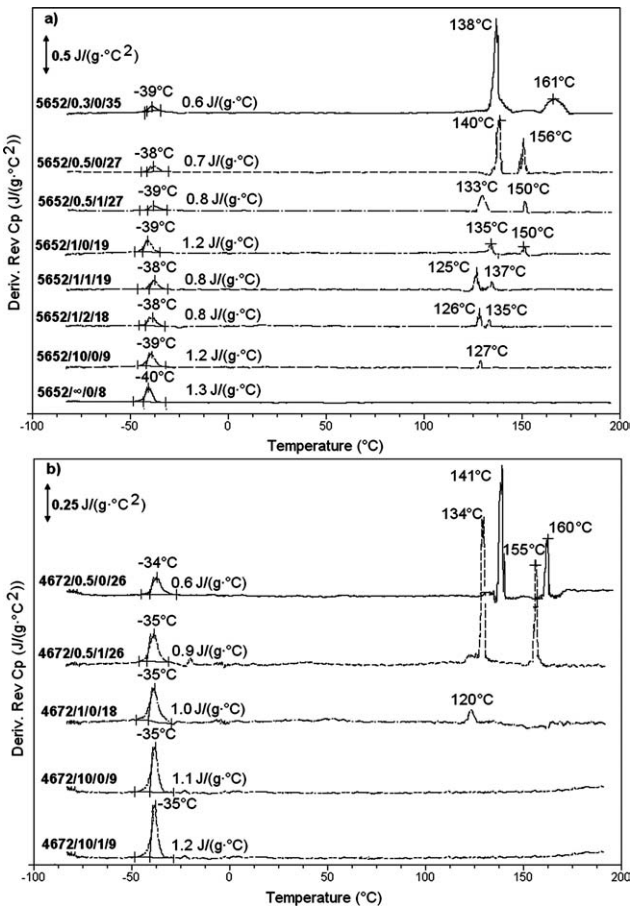

Figure 4. dC_p/dT signals vs. temperature for PUs and their nanocomposites with different HS content based on (a) 5652 and (b) 4672 macrodiol. (ΔC_p values are given at each individual curve; for sample code description, see Table I.)

An example of TMDSC experiment (with total, reversing and nonreversing heat flow) of semicrystalline sample 5652/0.3/0/35 is given in Figure 2.

Three endotherm regions have been detected: (i) glass transition of soft segments around −35°C, (ii) endotherm with minimum, T_{rel}, for all samples between 51 and 56°C and (iii) multiple endotherms in the temperature range from 120 to 175°C that are associated with gradual physical crosslink disruption.

While the first and the third are present in all three curves, the "middle" endothermic process is found only on curves of total and nonreversing heat flow vs. *T*, i.e., it is missing in reversing heat flow dependence. Various endotherms in this region have been found in similar PU systems and they have been attributed to different processes. The phenomenon will be discussed later in this chapter, together with results shown in Figure 4.

The influence of HSC and bentonite addition on thermal behavior of PC-PUs and PC-PU nanocomposites based on 5652 and 4672 macrodiols is shown in Figure 3(a) (5652) and 3(b) (4672 series). Data obtained from total specific heat flow vs. *T*

Table II. Thermal Properties of PC-PUs (Glass Transition Temperature of Soft Segments $(T_g)_{SS}$, Relaxation Temperature T_{rel}, Enthalpy of Relaxation ΔH_{rel}, Temperatures and Enthalpies of Melting Peaks T_{m1}, T_{m2}, ΔH_{m1}, ΔH_{m2}, Enthalpy of Fusion ΔH_m)

Sample code	$(T_g)_{SS}$ (°C)	T_{rel}, (°C)	ΔH_{rel}, (J/g)	T_{m1}, (°C)	T_{m2}, (°C)	$\Delta H_m = \Delta H_{m1} + \Delta H_{m2}$, (J/g)
5652/0.3/0/35	−39	53	8.7	138	161	43.4
5652/0.5/0/27	−38	56	7.2	140	156	29.7
5652/0.5/1/27	−39	53	0.6	133	150	25.1
5652/1/0/19	−39	55	10.2	135	150	23.4
5652/1/1/19	−38	51	5.8	125	137	18.9
5652/1/2/19	−38	52	7.2	126	135	14.5
5652/2/0/14	−39	51	10.3	127	-	3.6
5652/10/0/9	−40	53	3.5	-	-	-
4672/0.5/0/26	−34	55	12.0	141	161	28.4
4672/0.5/1/26	−35	54	2.1	134	155	26.2
4672/1/0/18	−35	54	8.4	121	-	8.1
4672/2/0/9	−35	56	4.6	-	-	-
4672/10/1/9	−35	56	2.2	-	-	-

dependences, shown in Figure 3, are summarized in Table II. From Table II follows that the value of enthalpy of relaxation, ΔH_{rel}, is (unlike ΔH_m values) almost independent on the composition for samples of both series with HSC $\geq$ 14 wt %, i.e., samples being either semicrystalline or highly organized but still amorphous (7–12 J/g). On the other hand, ΔH_{rel} decreases ($<$ 5 J/g) for highly amorphous systems (HSC $<$ 10 wt %). The addition of BO decreases ΔH_{rel} and ΔH_m in all cases compared to bentonite-free analogues. (For further details, see SAXS and WAXD experiments in. Ref. 22).

The degree of miscibility between hard and soft segments depends strongly on chemical composition of segments and also on the hard segment content.[25] In Figure 3, first transition is the glass transition of soft segments, $(T_g)_{SS}$ with the peak at −39°C ± 1°C for 5652-, and at ca. −35°C for 4672-based PUs. Neither HSC nor bentonite addition have significant influence on $(T_g)_{SS}$ position in all PUs tested. The degree of the microphase-separated structure can be analyzed from ΔT_g, i.e., the difference between T_g of the soft segment in PC-PUs, $(T_g)_{SS}$, and of the original PC diol, $(T_g)_{PCD}$. Higher value of ΔT_g evidences increasing miscibility due to favorable interaction between the soft and hard segments.[5] In both series, ΔT_g are quite small, ca. 10°C for 5652-, and 11°C for 4672-based PC-PUs, indicating strong microphase separation in all PC-PUs and PU nanocomposites prepared.

The endotherms above 125°C are assigned to a gradual disruption of physical crosslink and their multiple character can be a result of different domain sizes, or variable quality of ordering (varying content of perturbations in the crystalline structure).[26] The size and position of the melting endotherms have been shown to vary with the composition ratio and the lengths of the soft and hard segments.[27] Scattering experiments (SAXS and WAXD results in Ref. 22) were found to be very useful for the interpretation of thermal behavior in endotherm II region, which is closely connected with the degree of ordering/crystallization of HSD in both series: Reduction (or even disappearance) of multiple endothermic peak area of endotherm II in Figure 3 for higher R denotes the decrease of the HSD ordering degree: For 5652-based PUs, reduction of HSC from 35 to 14% led to the systematic ΔH_m decrease limiting 43.4 J/g (for semicrystalline 5652/0.3/0/35) to 3.6 J/g (for amorphous but highly organized 5652/0.5/0/14). For the amorphous sample with very limited organization (see Chapter SAXS, WAXD in Ref. 22), 5652/10/0/9, melting transition is not detected at all. A similar but more pronounced trend is observed for semicrystalline 4672-based PUs: by decreasing HS content from 26 to 18%, ΔH_m decreased from 28.4 J/g (4672/0.5/0/26) to 8.1 J/g (4672/1/0/18). Highly amorphous samples 4672/10/0/9 and 4672/10/1/9 did not show any melting region, which is in accordance with scattering results.[22] Temperatures of multiple endotherm peaks, T_{m1} and T_{m2}, decreased for all nanocomposites, as well as their enthalpy of fusion. Physical crosslink disruption at lower temperatures for BO-filled samples compared to BO-free analogues was similar to PC-PUs and their nanocomposites based on PC diols of MW 1000.[10] The reason for a small decrease might be the behavior of BO as an agent blending both hard and soft segment domains leading to their increasing miscibility. However, BO affinity to hard segments seems to be higher than that to soft segments, as detected by solid-state NMR spectroscopy and SAXS measurements.[22]

Direct information on the thermal transition processes can also be obtained from the temperature dependence of the reversing dC_p/dT signal, as shown in Figure 4 for 5652- and 4672-based series. Neither HSC nor bentonite addition have any significant influence on soft-segment glass transition temperature $(T_g)_{SS}$ (which is also visible from Figure 3), unlike differences of heat capacity ΔC_p, rinsing with soft segment contents, and hence disordering degree of HS. For example, ΔC_p double increased when compared semicrystalline sample 5652/0.3/0/35 (0.6 J/g/°C) and amorphous one 5652/∞/0/8 (1.3 J/g/°C).

The change of ΔC_p value by bentonite addition can be explained by the formation of intercalated layers which was confirmed by SAXS experiments.[22] For PU samples prepared at R = 0.5 (i.e., 5652/0.5/1/27, 4672/0.5/1/26), the addition of

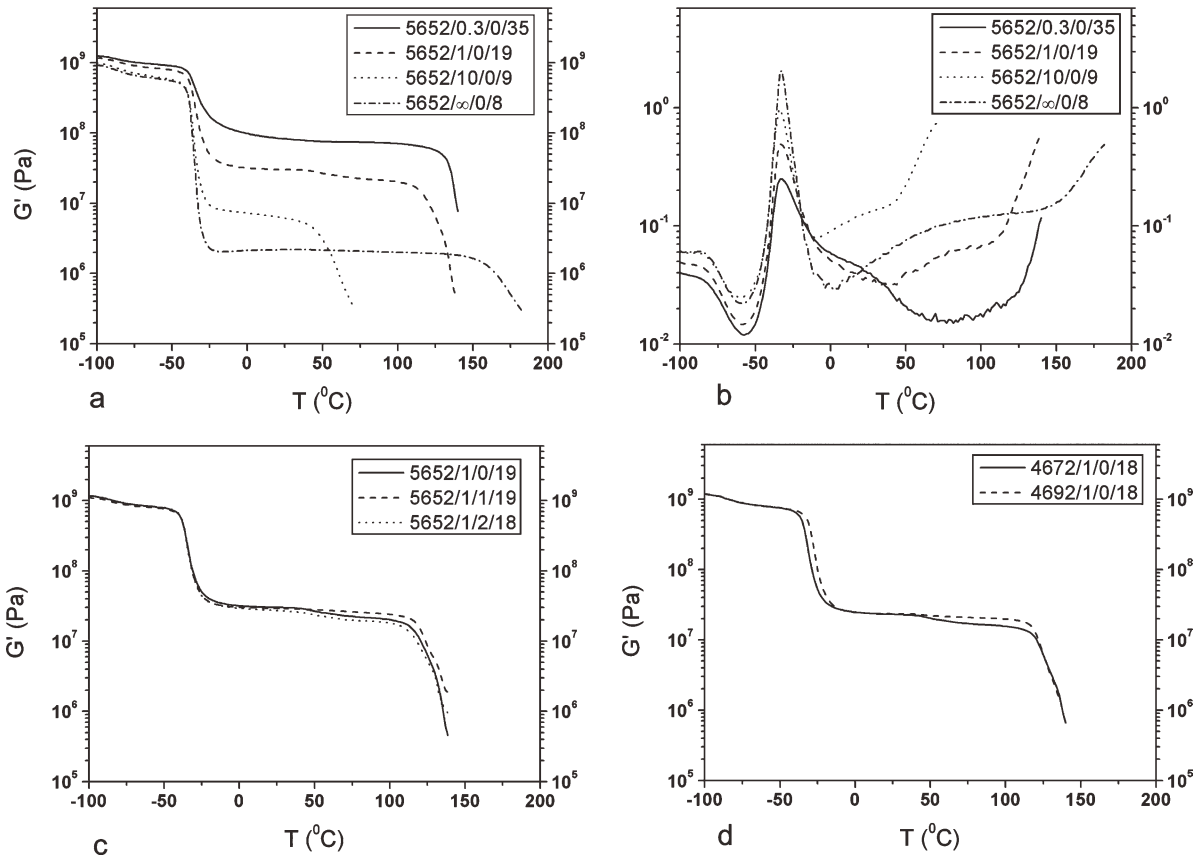

Figure 5. Shear storage modulus (G') vs. T (a, c, d) and tan (δ) vs. T (b) dependences. Series of 5652-based PC-PUs: influence of HS content (a, b), influence of bentonite concentration (c) and of C4/C6 ratio (d). (For sample code description, see Table I.)

bentonite caused the increase of ΔC_p (compared to their analogues, 5652/0.5/0/27 and 4672/0.5/0/26) indicating that all PU chains intercalated into the layers of the clays participated in the glass transition process.[‡] On the other hand: in samples prepared at $R = 1$, ΔC_p decreased by bentonite addition (cf. 5652/1/1/19 and 5652/1/2/18 vs. 5652/1/0/19), suggesting that the part of the PU chains intercalated into the filler layers did not participate in the glass transition process.[9] This difference is probably due to different degrees of ordering detected by scattering methods.[22] WAXD experiments confirm this assumption: A slight decrease of crystallinity degree (by 1 to 2%) was found in the case of both nanocomposites prepared at $R = 0.5$ compared to bentonite-free analogues, but the trend for $R = 1$ was quite opposite; the crystallinity degree increased by 4, respectively, by 5% in the case of the 5652-, respectively, 4672-based nanocomposites compared to their PC-PU analogues (for further details, see Table I and Figures 8 and 9 in Ref. 22).

Endothermic events between 40 and 75°C detected on curves of total and non reversing heat flow versus temperature in Figures 2 and 3 are not noticeable on the reversing dC_p/dT signal vs. T graph, similar to reversing heat flow vs. T diagram in Figure 2. The existence of diffused interfacial phase between SS and HS resulted from the order-disorder relaxation of the PU chain segments in the interface[9] or melting of noncrystalline hard-segment domains[5] in this region is suggested.

Thermal, thermomechanical and mechanical properties of samples 4672/1/0/19, 4692/1/0/19 and 4672/0.5/0/1/26 can be compared with results of PC-PUs 4672PU2, 4692PU2, and 4672PU3 studied in Ref. 5.[¶] PC-PUs mutually differ in the diisocyanate used (HDI vs. MDI[¶]) and technique of preparation (one-step vs. two-step prepolymerization technique[5]); but both hydroxyl components (PC macrodiol, BD), their ratio, and NCO index are the same.[¶] While ΔT_g in PC-PUs based on aromatic MDI depends on macrodiol/BD ratio (32.6°C for 4672PU2 and 27.8°C for 4672PU3),[5] both analogues PC-PUs based on aliphatic HDI, 4672/10/0/19 and 4672/0.5/0/26 have the same ΔT_g, ca. 11°C. This indicates higher phase separation and lower HSC sensitivity on phase mixing in HDI-based PC-PUs compared to MDI-based ones. The thermal stability of MDI-based PC-PUs was about 50°C higher than that of HDI-based ones [183.7°C (4672PU2) vs. 134/155°C (4672/1/0/19), and 207°C (4672PU3) vs. 141/160°C (4672/0.5/0/26)].

[‡]The same trend was observed for ratio $R = 10$.

[¶]The sample abbreviation in Ref. 5 means: first four numbers are the type of macrodiol, and the last number is the ratio $[NCO]_{prepolymer}/[OH]_{macrodiol}$. Last number: 2 corresponds to equimolar ratio of macrodiol and BD (i.e., our $R = 1$) and number 3 means double excess of OH groups of BD compared to macrodiol (i.e., our $R = 0.5$). Final [NCO]/[OH] ratio was 1.05 in all cases. Isocyanate used: 4,4′- methylene diphenyl diisocyanate (MDI).

Table III. Temperature of Glass Transition of Soft Segments, $(T_g)_{SS}$, Peak Values of Tan (δ) and G' Values at $T = (T_g)_{SS} + 60°C$

Sample code	$(T_g)_{SS}$ (°C)	Tan (δ) peak value	G′ at [$(T_g)_{SS}$ + 60°C] (MPa)
5652/0.3/0/35	−32.4	0.25	81.5
5652/0.5/0/27	−32.3	0.33	65.5
5652/1/0/19	−33.3	0.49	30.1
5652/1/1/19	−32.1	0.53	28.9
5652/1/2/18	−32.3	0.55	26.9
5652/2/0/14	−33.3	0.73	17.7
5652/10/0/9	−34.0	0.98	6.06
5652/∞/0/8	−32.4	2.06	2.19
4672/0.3/0/34	−29.3	0.30	72.5
4672/0.5/0/26	−29.2	0.35	61.9
4672/1/0/18	−29.0	0.55	22.8
4672/1/1/18	−29.2	0.62	22.2
4672/10/0/9	−29.4	1.08	5.22
4672/∞/0/8	−28.3	1.71	3.66
4692/1/0/18	−26.2	0.56	23.4

Dynamic Mechanical Thermal Analysis (DMTA)

The phase transitions (T_g, physical crosslink melting, and other) in the PC-PUs and nanocomposites and their effect on the mechanical properties of the products were further studied by dynamic mechanical thermal analysis (DMTA). Examples of the storage modulus G' and the loss factor tan(δ) as function of temperature are displayed in Figure 5, for the neat elastomers [Figure 5(a,b,d)] and for their nanocomposites with bentonite [Figure 5(c)]. DMTA results are summarized in Table III.

The shear storage modulus (G') vs. temperature dependences of all samples show a main glass transition near –33°C (5652 series) and –29°C (4672 series), associated with the soft macrodiol segment. Tan(δ) spectra display the main and most distinct peak at these abovementioned temperatures (–33 or –29°C for 5652 and 4672 series, respectively), corresponding to the mentioned step in G' spectra. This peak does not change its position with increasing HSC, only the height of the step in G' and the tan(δ) peak intensity increase with growing R, see Table III (the same trend was observed by TMDSC analysis for ΔC_p values; see Figure 4). In accordance with TMDSC results, the glass transition temperatures of soft segments, $(T_g)_{SS}$, do not depend on bentonite presence in both (4672- and 5652-) series. All $(T_g)_{SS}$ analyzed by DMTA—determined as $(\tan(\delta))_{max}$—are ca. 6°C higher than those determined by TMDSC. The DMTA spectra also show a small step in G' (and a small maximum of tan(δ)) near –75°C, which corresponds to a liberation of a part of the polycarbonate chains at this temperature.[16] The rubber plateau (G') covers a broad temperature region; it ranges from –20 up to +175°C, with the latter value decreasing with increasing R. Another small softening, i.e., G' modulus decrease in the rubbery region is observed at ca. 50°C; the intensity depends on R. Besides the most intensive process in PC-PUs at $R = 10$ (5652/10/0/9 and 4672/10/0/9), where the disruption of physical crosslinks is so strong that PC-PUs start to melt, the second most pronounced G' step occurs for $R = 1$ or 2 (5652/1/0/19, 5652/2/0/14 and 4672/1/0/18), unlike PC-PUs with the highest HSC (5652/0.3/0/35 and 4672/0.3/0/34) or the lowest HSC (5652/∞/0/8 and 4672/∞/0/8), where G' decrease is almost undetectable.

To get more information about G' modulus decrease in the rubbery region at around 50°C, additional DMTA experiment after the first run and cooling down the system was performed. In this purpose, the PU sample 5652/2/0/14 (with the most pronounced G' decrease in the first scan, featuring highly organized but still amorphous HSD; see Chapter SAXS and WAXD experiment in Ref. 22) was chosen. G' decrease at around 50°C was not registered in the second DMTA curve of investigated PC-PU, which is in a good agreement with our previous results.[16]

The final sample softening to linear polymer melt, during which all physical crosslinks disrupt (corresponding endotherm II in thermal analysis), takes place in the range of 100–200°C in all samples (with the above mentioned exception at $R = 10$). The samples with high hard segment content (5652/0.3/0/35 and 4672/0.3/0/34) are distinguished by rubber moduli more than one order of magnitude higher than samples with the lowest HSC (5652/∞/0/8 and 4672/∞/0/8). Interestingly, the samples 5652/10/0/9 and 4672/10/0/9 with very low contents HDI/BD units have stronger tendency to softening above 50°C than those with no butanediol extender and hence no HDI/BD units (5652/∞/0/8 and 4672/∞/0/8). The same trend was also observed in PC-PUs based on PC of MW ca. 1000 prepared recently.[16] Obviously, the simpler materials with R=∞ arrange easier and form more stable physical crosslinks, that is, particularly pronounced at T > 130°C; see Figure 5(a).

The choice of polycarbonate macrodiol, 5652, 4672, and 4692 and/or the presence of bentonite have not a big influence on the shape of the G' spectra of neat matrices and their composites [see Figure 5(a,c,d)]. The DMTA trends and profiles were fully analogous for all matrices.

Tensile Properties

The tensile properties (tensile strength, σ_b, elongation at break, ε_b, toughness,** Young's (E), M100 and M300 moduli) of PC-PUs and their nanocomposites were determined for all prepared samples. Three following dependences of tensile properties were studied: (i) the influence of the ratio R (i.e., HSC) of 5652- and 4672-based PC-PUs, (ii) the influence of bentonite and (iii) the influence of the macrodiol constitution. All tensile characteristics are summarized in Table IV.

1. The influence of the ratio R (i.e., HSC) in 5652- and 4672-based PC-PUs: The effect of the hard segment content (repeating HDI-BD sequences) on the trend in tensile properties was found to be very strong for both series studied [see Table IV and Figure 6(a)]. Elongations at break, ε_b, are very high for all samples prepared, spanning between 520 and 1123%, and they are mostly higher than 700%. Maxima ε_b values were achieved for $R = 10$ (1047% for 5652/10/0/9 and 1123% for 4672/10/0/9).

**Toughness is expressed as the energy necessary to break the sample per unit volume.

Table IV. Tensile Properties of 5652-, 4672-, and 4692-Based PC-PUs and Their Nanocomposites

Code	Tensile strength σ (MPa)	Elongation at break ε (%)	Young modulus *E* (MPa)	Modulus M100 (MPa)	Modulus M300 (MPa)	Toughness (mJ/mm^3)
5652/0.3/0/35	29.9	520	161.0	13.3	20.4	100
5652/0.4/0/30	55.6	737	117.1	12.0	20.0	198
5652/0.5/0/27	55.3	814	114.4	10.4	17.1	209
5652/0.5/1/27	39.7	651	95.9	9.1	15.5	125
5652/1/0/19	47.7	926	51.9	6.5	10.9	177
5652/1/1/19	43.1	753	47.2	6.0	11.0	133
5652/1/2/18	24.5	724	39.6	4.7	8.0	84
5652/2/0/14	47.9	704	25.4	4.5	9.1	117
5652/10/0/9	6.0	1047	0.3	0.9	1.0	28
5652/10/1/9	12.2	874	3.6	1.1	1.6	33
5652/∞/0/8	3.8	809	0.3	0.7	0.9	12
4672/0.5/0/26	45.1	866	105.4	10.6	16.5	204
4672/0.5/1/26	45.1	695	101.8	10.4	17.5	156
4672/1/0/18	53.4	992	34.1	7.0	11.7	216
4672/1/1/18	49.7	853	37.6	5.7	10.2	163
4672/2/0/13)	36.4	842	28.0	4.2	7.5	121
4672/10/0/9	14.9	1123	0.8	1.6	2.1	58
4672/10/1/9	17.8	976	0.5	1.5	2.1	53
4672/∞/0/8	24.5	808	1.0	2.2	3.8	63
4692/1/0/18	66.8	822	48.4	7.0	13.3	209

Tensile strengths values, σ_b, are distinguished by broader, more than one order span: from 3.8 MPa (5652/∞/0/8) up to 55.6 MPa (5652/0.4/0/30); 4672-based PUs feature by ca. 3 times narrower span than in 5652-based analogues. Toughness (expressed as the energy per unit volume necessary to break the sample) varied from 12 mJ/m^3 (5652/∞/0/8) to 216 mJ/m^3 (4272/1/0/18) also with the broader span of values for 5652-based PC-PUs (12 to 209 mJ/m^3) compared to 4672-based analogues (58 to 216 mJ/m^3). All moduli (Young, M100 and M300) decrease with increasing *R*. The difference in constitution (regularity) of macrodiol chain is possibly responsible for different tensile properties of samples containing less than 10 wt % of HS. All 4672-based PUs are composed only from even units: C4 (from macrodiol and BD) and C6 units (from HDI and macrodiol) unlike 5652-based samples being composed from the mixture of odd and even units: C4 (from BD), C5 (macrodiol) and C6 (HDI and macrodiol). The irregular C5 units of 5652 are almost certainly responsible for lower intensity (amount) of secondary bonds compared to 4672- based analogues, resulting in lower σ_b in the samples: Value σ_b of 4672/10/0/9 is 3 times higher than that 5652/10/0/9 and, in the case of $R = \infty$, where the chain extender (BD) is missing, (5652/∞/0/8 and 4672/∞/0/8), the multiple σ_b factor is even 5.25. On the other hand, if the PUs contain sufficient amount of HS (15% and higher; being either semicrystalline or containing highly organized, but still amorphous HSD; see WAXD and SAXS experiments in Ref. 22), the 4672- and 5652-based samples with identical ratio *R* show very similar tensile properties. In this case, the chain irregularity of 5652 can probably be fully balanced by its higher flexibility, so that the total strength of resulting secondary bonds is practically the same like in more regular, but stiffer chains of 4672 macrodiol. On condition that HSC is higher than 30%, S-shape course of the tensile curve (indicating strain-induced crystallization) is missing in both series, which is connected with σ_b and ε_b decrease.[††]

2. Influence of bentonite: (1 wt % addition) was tested in both series for $R = 0.5$, 1 and 10 (i.e., 5652/0.5/0/27 vs. 5652/0.5/1/27, 4672/0.5/0/26 vs. 4672/0.5/1/26, etc.). In all cases, the elongation at break is reduced in BO-containing samples (mostly by 20%), compared with BO-free analogues. Toughness and σ_b values depend on *R*; the differences are more pronounced in 5652-series: At higher HSC (5652/0.5/0/27 vs. 5652/0.5/1/27), the presence of BO deteriorates σ_b (by ca. 30%) and toughness by ca. 40%, but for $R = 10$, σ_b is ca. 2 × higher, and toughness is higher by ca. 20% in 5622/10/1/9 compared to 5652/10/0/9. All tensile properties are substantially deteriorated by the addition of 2 wt % of BO; tested only for 5652 macrodiol and at ratio $R = 1$ (5652/1/2/18).[‡‡] Figure 6(b) shows stress-strain dependences of PC-PUs and PU nanocomposites of 5652-based samples prepared at $R = 1$ and 10.

[††]The stress-strain curves of PC-PUs and PC-PU nanocomposites were described into details in our previous paper.[16]

[‡‡]We were unable to prepare PU nanocomposite with 5 wt % of BO due to the full loss of elastomeric properties.

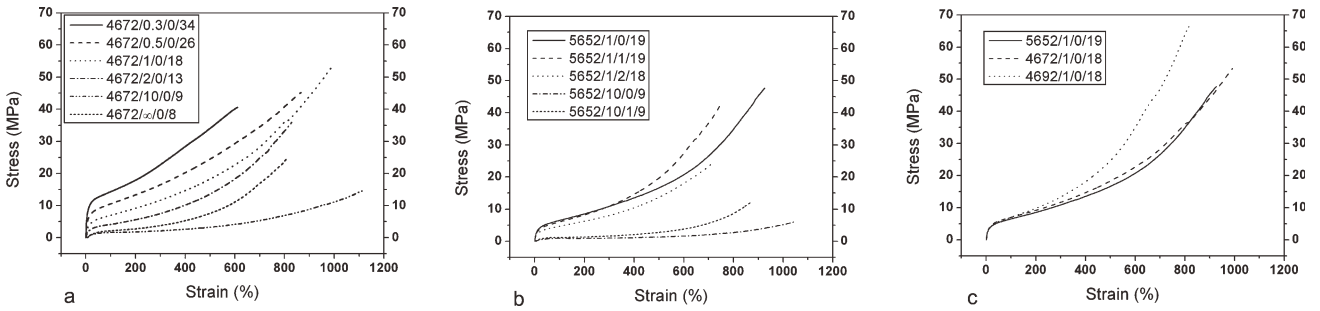

Figure 6. Stress-strain dependences for 4672-based PC-PUs (a), 5652-PC-PUs and their nanocomposites prepared at $R = 1$ and 10 (b) and the influence of macrodiol constitution on tensile properties at $R = 1$ (c). (For sample code description, see Table I.)

3. To test the influence of macrodiol constitution (and hence chain regularity) on tensile properties, PC-PUs made from 5652, 4672 and 4692 macrodiol at $R = 1$ were prepared and compared. Their stress-strain dependences are shown in the Figure 6(c). As all elastomers were prepared by identical procedure, and they content practically identical amount of HDI and BD, the differences in tensile properties have to issue from the differences in macrodiol: constitution and regularity. 4672/1/0/19 and 5652/1/0/19 have very similar course the whole stress-strain curve, but the course of 4692/1/0/18 is different: At lower ε (up to ca. 200%), the 4692-course is similar to the others ($\Delta\varepsilon <$ 15%), but then, in the region of strain-induced crystallization, and especially for $\varepsilon > 400\%$, σ_{4692} is higher: by ca. 35 to 40% for $\varepsilon > 600\%$, and by ca. 45% at $\varepsilon > 800\%$ compared to 4672- and 5652-based PUs. The efficiency of strain-induced crystallization is dependent on the symmetry of chemical structure, which is closely related to the regularity of packing of the soft segments.[28] Thus, PU prepared from the most regular 4692 macrodiol had the highest σ_b. However, the more efficient strain-induced crystallization of 4692-based sample was accompanied at the same time by reducing ε_b compared to less regular macrodiols 4672 and 5652, resulting in very close toughness values of all PU samples (209 to 219 mJ/mm^3).

As the toughness can be taken as the quality criterion of PUs prepared, dependences of the toughness on HSC, NCO group content and content of OH groups in BD were also investigated. They are shown in Figure 7 together with results of PUs based on macrodiols of MW 1000, $(PC\text{-}PUs)_{1000}$, published recently.[16] Both 5652- and 4672-based PUs dependences $(PC\text{-}PUs)_{2000}$ have the same trend, with high and very similar tensile strength and toughness in the region of ca. 1.3 to 2.75 mmol NCO groups/g, ca. 0.75 to 1.75 mmol/g OH groups in BD which corresponds ca. 15 to 30% of HSC. If compared $(PC\text{-}PUs)_{2000}$ with $(PC\text{-}PUs)_{1000}$, the influence phase separation/phase mixing on tensile properties of clearly detected. Shorter macrodiol chains lead to higher PU phase-mixing, so that the microphase separation in $(PC\text{-}PUs)_{1000}$ is weaker than in $(PC\text{-}PUs)_{2000}$ analogues. Comparable values of the toughness of $(PC\text{-}PUs)_{1000}$ and $(PC\text{-}PUs)_{2000}$ were achieved only for comparable contents of OH groups in BD. For comparable NCO groups/g or HSC, higher toughness values was achieved in $(PC\text{-}PUs)_{2000}$ than for $(PC\text{-}PUs)_{1000}$ analogues up to HSC ca. 25% (NCO content $<$ 2.5 mmol/g). At higher HSC or NCO amount $(PC\text{-}PUs)_{2000}$ start loose both the elasticity and the tensile strength unlike $(PC\text{-}PUs)_{1000}$ analogues.

Tensile properties of samples 4672/1/0/18, 4672/0.5/0/26 and 4692/1/0/18 can be compared with samples 4672PU2, 4672PU3 and 4692PU2[¶] in Ref. 5. Samples made from MDI[5] have substantially lower ε_b and σ_b than HDI-based analogues. Aliphatic HDI chain feature more flexible character than more rigid MDI (possible reason for increased elongation). Better flexibility and higher phase separation of HDI-based PU chains can be the reason for higher tensile strength in comparison to MDI-based PC-PUs.

Gas transport Properties

The influence of HS content, of the constitution of PC chain and of the presence/absence of bentonite on gas transport properties (GTP) in PC-PUs and their nanocomposites was studied. Permeabilities (P) in Barrers, diffusion coefficients, (D) in m^2/s, solubilities (S) in mol/m^{3}Pa and selectivities are summarized in Table V (influence of PC constitution and presence/absence of BO) and Figure 8 (influence of HS content for the T5652-based series). Permeability correspond in most cases to units of Barrers, solubility (S) is in the order 10^{-5} mol/m^3 Pa, diffusion coefficients are in order 10^{-11} m^2/s, and selectivities of industrially interesting gas pairs varies from 2 to 38. Values of P, S and D of CO_2 are mostly one order of magnitude higher than those for other gases. All studied GTP depend on the constitution of PC chain; in almost all cases the lowest values of permeability, diffusion coefficient, solubility and selectivity are found for PU made from (the most regular) 4692 macrodiol, and the highest values for (the most irregular) 5652 one (cf. GTP values of 4692/1/0/19, 4672/1/0/19 and 5652/1/1/19 in Table V). That means that the organization of individual building units, their ratio and the degree of the chain arrangement in polycarbonate chain affect the gas transport properties. On the other hand, GTP are not almost affected by the presence of 1 wt % BO (cf. 5652/1/0/19 and 5652/1/1/19 in Table V). The influence of HS

[¶]The sample abbreviation in Ref. 5 means: first four numbers are the type of macrodiol, and the last number is the ratio $[NCO]_{prepolymer}/[OH]_{macrodiol}$. Last number: 2 corresponds to equimolar ratio of macrodiol and BD (i.e., our $R = 1$) and number 3 means double excess of OH groups of BD compared to macrodiol (i.e., our $R = 0.5$). Final [NCO]/[OH] ratio was 1.05 in all cases. Isocyanate used: 4,4′- methylene diphenyl diisocyanate (MDI).

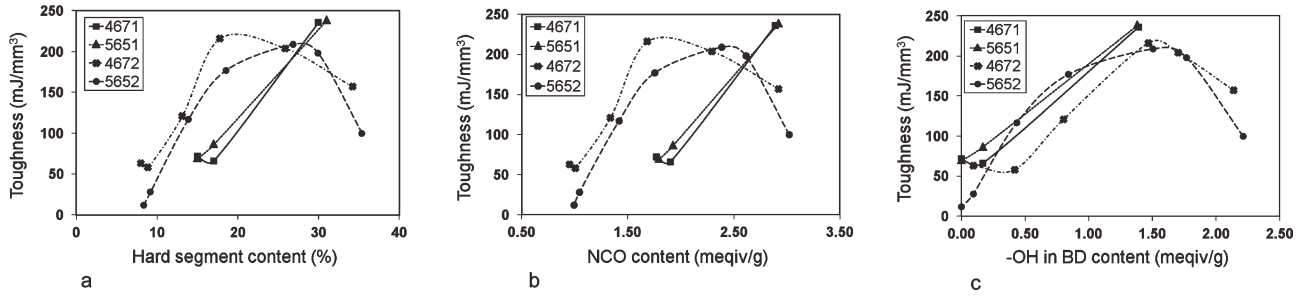

Figure 7. Toughness dependences on hard-segment content (a), concentration of isocyanate groups (b), and concentration of hydroxyl groups in chain extender (c). Series 5652 and 4672 are compared with 5651- and 4671-based ones.[16] (For sample code description, see Table I.)

content on GTP was tested for the most irregular, 5652-based PUs. The results are given in Figure 8. Values of permeability and diffusion coefficient gradually decrease with the increasing contents of HS. As concerns the solubility and selectivity, the trend is not so pronounced and differences are rather small. The differences are at the limit of experimental errors, but we can conclude that, without any doubts, the samples 5652/1/0/19 or 5652/2/0/14, i.e., the PU samples with excellent tensile properties provide high solubility and selectivity for common gases as compared with other prepared and studied samples.

For all samples tested, permeability decreases in sequence: CO_2, H_2, O_2, CH_4, and N_2; diffusion coefficient in sequence: H_2, O_2, N_2, CO_2, and CH_4; and solubility in sequence: CO_2, CH_4, O_2, N_2, and H_2. Values of the separation factor (selectivity) were determined for interesting industrial gas pairs such as CO_2/N_2, CO_2/CH_4, H_2/CH_4, and O_2/N_2; the lowest values were found for O_2/N_2, and the highest for CO_2/N_2 pairs (one order of the magnitude difference) and they are practically independent on HSC.

Further we studied the effect of hard segments on GTP (Figure 8): Permeabilities and diffusion coefficients of all gases decrease with increasing hard segment content. The values of gas solubility are nearly constant at lower content of hard segment (9 to 19%); the differences are in a range of experimental errors. Only a fairly high content of hard segments (35%) caused a slight decrease in solubility of all gases. Because the gas flow occurs predominantly through the soft segments, increasing content of hard segment does not affect the separation properties of materials significantly.

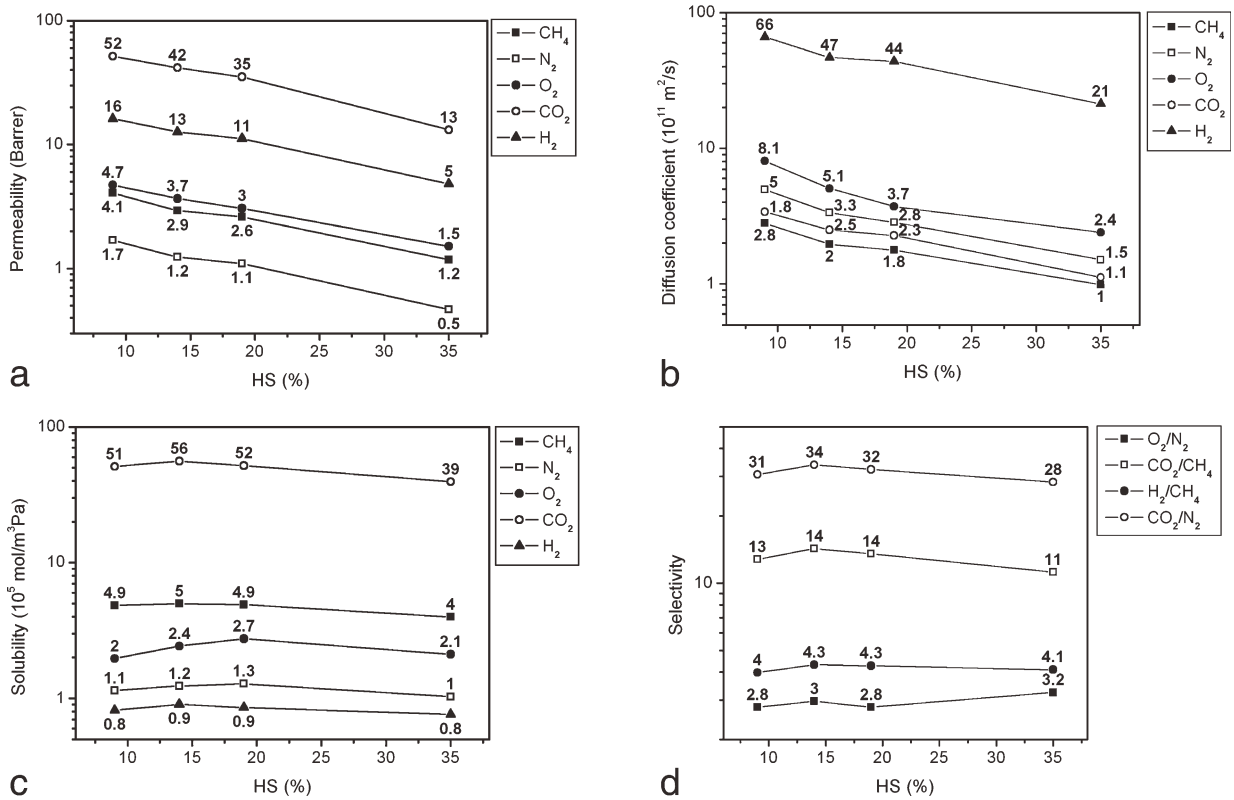

Figure 8. Gas transport properties of PC-PUs. The influence of HSC in 5652-based PC-PUs. (For sample code description, see Table I.)

Table V. Gas Transport Properties of PC-PUs and PC-PU Nanocomposite

	Permeability (barrer)[a]				
Composition	CH_4	N_2	O_2	CO_2	H_2
4692/1/0/18	1.3	0.8	2	21	7.1
4672/1/0/18	1.6	0.7	2.3	26	8.4
5652/1/0/19	2.6	1.1	3.1	35	11.1
5652/1/1/19	2.7	1.1	3.1	35	11.1

	Diffusion coefficient $10^{11}(m^2/s)$				
Composition	CH_4	N_2	O_2	CO_2	H_2
4692/1/0/18	1.1	2.8	3.6	1.3	33
4672/1/0/18	1.3	2	4.2	1.5	36
5652/1/0/19	1.8	2.9	3.7	2.3	44
5652/1/1/19	1.8	3.3	4.8	2.4	43

	Solubility $10^5(mol/m^3\ Pa)$				
Composition	CH_4	N_2	O_2	CO_2	H_2
4692/1/0/18	3.9	0.9	1.8	52	0.7
4672/1/0/18	4.2	1.2	1.9	60	0.8
5652/1/0/19	4.9	1.3	2.8	52	0.9
5652/1/1/19	5	1.1	2.2	50	0.9

	Selectivity			
Composition	O_2/N_2	CO_2/CH_4	H_2/CH_4	CO_2/N_2
4692/1/0/18	2.5	15.9	5.5	26
4672/1/0/18	3.4	16.3	5.3	38
5652/1/0/19	2.8	13.5	4.3	32
5652/1/1/19	2.8	13.3	4.2	32

[a] 1 barrer = 10^{-10} cm^3 (STP) cm/(cm^2 s cm Hg).

Effect of the macrodiol composition on GTP was also studied: Values of permeability of all gases increase in sequence 4692, 4672 and 5652 due to increasing disorder of macrodiols and increasing flexibility and hydrophobicity of chains containing more CH_2 units (on average 72, 74 and 77 CH_2 units in 4692, 4672 and 5652 samples, respectively). Apparently, the high solubility and low diffusion coefficient of CH_4 and CO_2 can be attributed to favorable interactions with the polycarbonate part of PU chain and with its CH_2 groups. The lower separation factors of 5652-based PUs may be caused by less ordered arrangement of its chain.

According to our knowledge, gas transport properties of given materials are not described in literature yet. For this reason we prepared membranes from two commercial PU materials, and compared their GTP data with results of PC-PUs and PU nanocomposites. ZWALUW is aromatic-based PU usually used as seal assembly foam. Permeabilities of all measured gases of ZWALEW membrane are several times lower in comparison with our studied materials ($P(CH_4)$: 0.14, $P(N_2)$:0.23, $P(O_2)$: 0.44, $P(CO_2)$: 0.94 and $P(H_2)$: 2,34 Barrer) and the separation coefficients for selected gas pairs are different (CO_2/N_2: 4.15, CO_2/CH_4: 6.83, H_2/CH_4: 16.96 and O_2/N_2: 1.92). The commercially produced poly(carbonate urethane), PCU, Aldrich No. 418323 is based on poly(1,6-hexyl-1,2-ethyl carbonate) diol, 4,4′-methylenebis(phenyl isocyanate) and 1,4-butanediol, so that PCU more closely resembles our PC-PUs. While PCU permeability values are 4 to 5 times lower than that obtained for PC-PUs: ($P(CH_4)$: 0.32, $P(N_2)$: 0.15, $P(O_2)$: 0.53, $P(CO_2)$: 4.75 and $P(H_2)$: 3.02 Barrer), separation coefficients for CO_2/N_2 (32.09), CO_2/CH_4 (14.89), H_2/CH_4 (9.48) and O_2/N_2 (3.58) gas pairs are similar. As GTP influence of macrodiol constitution in PC-PUs was found not to be significant, the lower PCU permeabilities can be caused by the presence aromatic diisocyanate, which is more rigid than aliphatic one and MDI products could be much bigger gas "barrier" than more flexible HDI-based PC-PUs.

CONCLUSIONS

Thermal, thermomechanical, mechanical and gas transport properties of PC-PUs and their nanocomposites depend almost exclusively on the hard segment contents; the influence of the macrodiol chain and the presence of 1 wt % of nanofiller were found insignificant. The impact of the chain constitution of polycarbonate diols 5652, 4672 and 4692 on the end-use properties of polyurethane products was found unimportant. It was found that bentonite at low concentration of 1 wt % is well incorporated in the polyurethane matrix. Detailed study (performed in this and in previous paper[22] indicates that BO is as an efficient nanofiller, which acts as an agent blending the hard and soft segment domains.

Three thermal transitions were detected by TMDSC and DMTA. The first one (–30 to –40°C), corresponding to the glass transition of soft segments neither depends on hard segment content nor on the presence of bentonite. The second transition, well detectable at all irreversible thermal curves (TMDSC) and in the first scan (DMTA), is located at the temperature region 50 to 55°C. The third transition, located at T higher than 100°C, is a disruption (melting) of highly organized (crystalline) hard segment domains, i.e., the disruption of hydrogen bonds and other physical crosslinking bonds inside these domains. All PC-PUs and their nanocomposites are stable up to 125°C, with the exception of the samples prepared with very low contents (2 wt %) of BD, where complete disruption of physical network joints occurs at ca. 75°C. Samples with the broadest span of rubbery plateau (almost 200°C) are PC-PUs prepared without any chain extender.

The formation of a sufficient amount of reasonably strong secondary bonds resulting in excellent tensile properties of PC-PUs depends both on the flexibility and regularity of the polycarbonate building units. The influence of macrodiol chain regularity on tensile properties of PC-PUs is more pronounced in systems containing less than 10 wt % of hard segments.

Very high values of permeability, solubility and diffusion coefficient for CO_2 are caused by favorable interactions of CO_2 with carbonate units in PC-PU. Presence of 1 wt % of BO does not practically affect gas transport properties of PU nanocomposites.

To summarize, in this article, we investigated and confirmed an important effect of the internal arrangement of PU chains spanning from the segmental up micrometer level (which we detected recently and studied in detail by spectroscopy, microscopy and scattering methods) on the macroscopic properties. For the application, e.g., as topcoats or films, polycarbonate-based polyurethanes containing 18 to 26 wt % of hard segments feature the best combination of end-use properties tested.

ACKNOWLEDGMENTS

The authors from IMC wish to thank the Grant Agency of the Czech Republic (Czech Science Foundation, project No. P108/10/0195) for financial support of this work. The project of Serbian Ministry of Education and Science (No. 45022) is appreciated as well.

REFERENCES

1. Boyce, Y. J.; Lee, M. C.; Balizer, G. F. E. *Polymer* **2006,** *47*, 319.
2. Koberstein, J. T.; Galambos, A. F.; Leung, T. M. *Macromolecules* **1992,** *25*, 6195.
3. Seymour, R. W.; Cooper, S. L. *Macromolecules* **1973,** *6*, 48.
4. Seymour, R. W.; Cooper, S. L. *J. Polym. Lett.* **1971,** *9*, 689.
5. Kojio, K.; Nonaka, Y.; Masubuchi, T.; Furukawa, M. *J. Polym. Sci. Polym. Phys.* **2004,** *42*, 4448.
6. Kultys, A.; Rogulska, M.; Pikus, S. Skrzypiec, K. *Eur. Polym. J.* **2009,** *45*, 2629.
7. Hesketh, T. R.; Van Bogart, J. W. C.; Cooper, S. L. *Polym. Eng. Sci.* **1980,** *20*, 190.
8. Eisenbach, C. D.; Baumgartner, M.; Gutner, C. In Advanced in Elastomers and Rubber Elasticity; Lai, J.; Mark, J. E.; Eds.; Plenum Pr., New York, **1986; p 15.**
9. Jin, J.; Song, M.; Yao, K. *J. Thermochim. Acta* **2006,** *447*, 202.
10. Pavličević, J.; Špírková, M.; Strachota, A.; Mészáros Szécsényi, K.; Lazić, N.; Budinski-Simendić, J. *Thermochim. Acta* **2010,** *509*, 73.
11. Finnigan, B.; Mattin, D.; Halley, P.; Truss, R.; Campbell, K. *Polymer* **2004,** *45*, 2249.
12. Qiu, Z.; Ikehara, T.; Nishi, T. *Polymer* **2003,** *44*, 3095.
13. Narine, S. S.; Kong, X. H.; Bouzidi, L.; Sporns, P. *J. Am. Oil Chem. Soc.* **2007,** *84*, 55.
14. Waterlot, V.; Couturier, D.; Waterlot, C. *J. Appl. Polym. Sci.* **2011,** *1742*, 119.
15. Bil, M.; Ryszkowska, J.; Wozniak, P.; Kurzydlowski, K. J.; Lewandowska-Szumiel, M. *Acta Biomater.* **2010,** *6*, 2501.
16. Špírková, M.; Pavličević, J.; Strachota, A.; Poreba, R.; Bera, O.; Kaprálková, L.; Baldrian, J.; Šlouf, M.; Lazić, N.; Budinski-Simendić, J. *Eur. Polym. J.* **2011,** *47*, 959.
17. Kojio, K.; Furukawa, M.; Motokucho, S.; Shimada, S.; Sakai, M. *Macromolecules* **2009,** *42*, 8322.
18. Tanaka, H.; Kunimura, M. *Polym. Eng. Sci.* **2002,** *42*, 133.
19. Kojio, K.; Nakamura, S.; Furukawa, M. *J. Polym. Sci. Polym. Phys.* **2008,** *46*, 2054.
20. Kultys, A.; Rogulska, M.; Gluchowska, H. *Polym. Int.* **2011,** *60*, 652.
21. Špírková, M.; Strachota, A.; Urbanová, M.; Baldrian, J.; Brus, J.; Šlouf, M.; Kuta, A.; Hrdlička, Z. *Mater. Manuf. Process* **2009,** *24*, 1214.
22. Špírková, M.; Poręba, R.; Pavličević, J.; Kobera, L.; Baldrian, J.; Pekárek, M. *J. Appl. Polym. Sci,* **2012**, DOI 10.1002/app.36993.
23. Daniel-Da-Silva, A. L.; Bordado, J. C. M.; Martin-Martinez, J. M. *J. Polym. Sci. Polym. Phys.* **2007,** *45*, 3034.
24. Schauer, J.; Sysel, P.; Maroušek, V.; Pientka, Z.; Pokorný, J.; Bleha, M. *J. Appl. Polym. Sci.* **1996,** *61*, 133.
25. Lazić, N. L.; Budinski-Simendić, J.; Ostojić, S.; Kicanović, M.; Plavsić, M. B. *Mater. Sci. Forum* **2007,** *555*, 473.
26. Kim, Y. S.; Lee, J. S.; Ji, Q.; McGrath, J. E. *Polymer* **2002,** *43*, 7161.
27. Wang, L. F. *Eur. Polym. J.* **2005,** *41*, 293.
28. Mishra, A.; Aswal, V. K.; Maiti, P. J. *Phys. Chem. B* **2010,** *114*, 5292.